JOURNAL OF Applied Polymer SCIENCE

Morphology, Microstructure, and Electrical Properties of Poly(D,L-lactic acid)/Carbon Nanocapsule Composite Nanofibers

Huan-Sheng Chien, Chi Wang
Department of Chemical Engineering, National Cheng Kung University, Tainan 701, Taiwan, Republic of China
Correspondence to: C. Wang (E-mail: chiwang@mail.ncku.edu.tw)

ABSTRACT: The morphologies and properties of poly(D,L-lactic acid)/carbon nanocapsule (CNCs) electrospun fiber mats were studied. To determine the effect of filler, a solution without sufficient entanglement density was used. The rheological results showed that the solution entanglement density was enhanced by the addition of filler, which led to the formation of network between the polymer chains and filler particles. The findings can be used for further exploration of electrospinning in semidilute solutions. The electrical conductivities of electrospun fiber mats and cast films were determined and fitted using the percolation theory. When the CNC content was above the critical percolation concentration, a master curve was obtained provided that the conductivity curves were normalized with the level of percolation network. The porosity effect was investigated. In addition, the microstructure of as-spun composite fiber was examined in detail. © 2012 Wiley Periodicals, Inc. J. Appl. Polym. Sci. 000: 000–000, 2012

KEYWORDS: electrospinning; entanglement; filler; percolation

Received 16 January 2012; accepted 27 May 2012; published online
DOI: 10.1002/app.38116

INTRODUCTION

Electrospinning is a powerful technique for producing polymer nanofibers with diameters ranging from the micro- to the nanometer scale, depending on the solution properties (i.e., viscosity, conductivity, and surface tension) and processing parameters (i.e., flow-rate, applied voltage, and working distance).[1,2] In recent years, some useful electrospinning devices were developed for producing nanofibers.[3,4] In electrospinning process, the presence of sufficient chain-entanglement density in the working solution is a prerequisite for fiber formation. Because it enhances the development of a deformable network, therefore, preventing capillary breakup. In other words, there is a minimum concentration (c_e) below which the entanglements of polymer chains are absent and electrospinning will degenerate into electrospraying.[5–7] In solution electrospinning, solution viscosity can be regarded as the most important factor in determining the morphology of electrospun products. Solution viscosity is considered the most important solution property in determining fiber diameter; the fiber diameter decreases with decreasing solution viscosity.[8–10] Higher solution conductivity is also required to acquire thin fibers. Based on these two aforementioned facts, two approaches are usually used to reduce as-spun fiber diameter. The first approach is to increase solution conductivity by adding soluble salt or a more conductive solvent.[2,8–12] However, the addition of salt and solvent complicates the electrospinning process, and the obtained fiber mats need to be purified to remove the salt. The second approach is to reduce solution viscosity by increasing the solution temperature. However, this method is limited to a solution that has sufficient high-entanglement density for obtaining smooth electrospun fibers.[13–16]

In this study, we propose another method for preparing ultrafine electrospun fibers. The addition of insoluble filler using carbon nanocapsules (CNCs) is proposed to enhance the development of the entangled network structure in a prepared semidilute solution. Some studies have been reported that the addition of filler enhances the solution viscosity.[17,18] Electrospun products with a relatively smooth fiber shape can thus be obtained. CNCs are polyhedral nanoscale particles consisting of a concentric graphene-layered structure with a cavity in the center.[19,20] They are considered materials with properties between those of fullerene and carbon nanotubes (CNTs). CNT have a high aspect ratio ($>10^2$), whereas CNC, which is considered a special type of CNT, have a lower aspect ratio ($\sim$2).[21]

CNTs have been extensively studied because their polymer composites have superior electrical and mechanical properties combined with very high aspect ratios.[22–28] Such as CNT was added to polystyrene (PS),[25] polyethylene oxide (PEO),[26,27] and poly(-lactic acid) (PLA)[28] electrospun fiber mats. However, previous studies on composite fibrous mats highlighted the need for adequate dispersion of CNT filler in the matrix to enhance the physical properties; even the prepared composite solution had a very low CNT content. Dror et al.[23] dispersed CNTs with gum

arabic as an additive to create a colloidal suspension of CNTs in the solution. Gum arabic prevented CNTs from aggregating before electrospinning. Dubois and coworkers[25] proposed the use of a copolymer as an interfacial agent to modify the dispersion of CNTs. Compared to CNTs, CNCs have a much lower aspect ratio, which may lead to good dispersion in prepared solutions.

Few studies have been conducted on granular material conduction behavior in composites, specifically in fibrous electrospun nonwoven composites.[29] In addition to CNTs, graphenes and carbon blacks were often used as conducting fillers. However, the conducting nature of these raw materials was quite different. Many studies have been conducted on CNT-filled polymer composite fiber mats, whereas limited studies have been conducted on the performance of CNC-filled polymer composite fibers. CNC can be regarded as a special type of CNT to have a lower aspect ratio. In our work, CNCs were used to prepare composites with different morphologies, such as fiber mats and cast films. Because of the similar conductive nature, the electrospun fiber mats provide a good example for a fair comparison with the cast film. The second part of this work was motivated by the lack of reported studies on the percolation conduction behavior of deformable fibrous mats containing nanosize conducting particles, such as CNCs.

Poly(D,L-lactic acid) (PDLLA) is widely used in various biomedical applications, such as in implant devices, tissue scaffolds, and internal sutures, due to its biodegradability and biocompatibility.[30,31] PDLLA is a compostable polymer derived from renewable sources. The preparation of thinner fibers with a large specific surface area is important for its end applications. Solution electrospinning is the process preferred by many because the fibers are readily obtained without damaging the polymers.[32–34] Compared to the formation of single-phase fibers, that of composite fibers allows additional design freedom, meaning that the physical properties of the fibers can be tailored as required by specific applications. This is another consideration for investigating the effects of filler on the preparation of PDLLA composite fibers.

The effects of filler on the semidilute PDLLA solution rheology and electrospinning process are investigated in this study. The preparation of ultrafine electrospun composite fibers that have a high specific surface area is presented. Findings from the study can be used for further exploration of electrospinning in semidilute solutions, especially with regard to adding filler to polymer solutions. This allows for the creation of novel composite fibers that can be used in the development of functional substrates for a variety of applications, ranging from electrical sensors to matrices for tissue engineering, to be more flexible. The results illustrate a close relationship between the PDLLA/CNC solution rheology and the morphology of electrospun products. We demonstrate the effect of filler on the microstructure of as-spun composite fibers. The conduction behavior of a PDLLA/CNC composite fiber mat is also investigated.

EXPERIMENTAL

PDLLA/CNC Solution Preparation and Properties

PDLLA pellets (D-lactide content: 10%) with a molecular weight of 1.78×10^5 g/mol (code number: 8300 D, Nature Work) were obtained. Surface-modified CNCs, produced using the pulse plasma arc-discharge method,[19,20] were provided by the Industrial Technology Research Institute (ITRI). HPLC-grade dimethyl formamide (DMF) purchased from J.T. Baker was used as the solvent to prepare the polymer solutions with various concentrations for electrospinning. Densities of the PDLLA and CNC are 1.23 and 1.60 g/cm^3, respectively.

In preparing the homogenous PDLLA/CNC solution with various CNC loadings, a PDLLA/CNC composite with a desired composition was prepared using the following procedure to ensure that CNCs dispersed well in the prepared solution. Weighted CNC filler was first added into the DMF solvent, followed by ultrasonic treatment for 3 h. The weighted PDLLA polymer was then added to prepare a homogeneous dilute solution. The suspension solution with a solid content of 1% (w/v) was then precipitated in a 10-fold excess volume of methanol. The obtained powders were dried in a vacuum oven until the residual solvent was removed. The as-prepared composite with a desired composition was dissolved in the DMF to prepare the PDLLA/CNC solutions.

The surface tension (γ), and conductivity (κ) of the prepared solutions were measured using Face surface tension meter (CBVP-A3), and Consort conductivity meter (C832), respectively. The viscoelastic properties of the solutions were measured in a strain-controlled rheometer (ARES, TA Instruments) using a cup-and-bar feature at room temperature.[35] The oscillatory shear mode was used to determine the storage modulus $G'(\omega)$ and loss modulus $G''(\omega)$ over a range of frequencies, ω, at room temperature. The solution complex viscosity (η^*) was derived from the dynamic properties using:[35] $[(G'/\omega)^2 + (G''/\omega)^2]^{0.5}$.

Preparation of Electrospun PDLLA Fibers Containing CNC Filler

A solution (i.e., 13 wt % solution) without sufficient entanglement density was used to monitor the effect of filler on the as-spun fiber morphology; solutions with various amounts of CNC filler, ranging from 1 to 5 wt % (based on the total weight of PDLLA solution), were prepared. All prepared solutions were then subjected to room temperature electrospinning, in which the needle size was D_i/D_o/length = 1.07/1.47/40.0 mm, where D_i and D_o are the inner and the outer diameters of the needle, respectively. The composite fibers were prepared by electrospinning 13 wt % PDLLA solutions, which had various amounts of CNCs. To prepare the conducting fiber mat, more CNC filler (up to 13 wt %) was added to the PDLLA solution (the composition of the PDLLA/CNC composite fibers was up to 1/1 in w/w).

Electrospun Fiber Characterization

The morphology of the fibers was observed under a scanning electron microscope (SEM, Hitachi S4100). The fiber diameters were measured from a collection of $\sim$ 500 fibers, from which the average diameter of fiber (d_f) and bead (D) portions were determined. Thermograms were obtained using a differential scanning calorimeter (DSC) (Perkin–Elmer, DSC7) under a nitrogen atmosphere at a scanning rate of 10°C/min. Crystallinity values were determined using the ratio of $\Delta H_m/\Delta H_f$, where ΔH_m and ΔH_f are the measured heat of fusion and the heat of

fusion for a 100% PDLLA crystal, respectively. A value of $\Delta H_f = 93.7$ J/g was used to calculate the degree of crystallinity.[30] A rotating-anode X-ray generator (Rigaku, Dmax2000) with a mono-chromatized Cu K_α beam was used to obtain the wide-angle X-ray diffraction (WAXD) intensity profile of the samples. A transmission electron microscope (TEM, Joel JEM-1200EX) was used to determine the locations of CNC particles in the nanofibers.

Electrical Property Measurements

Two different types of sample were prepared for the electrical conductivity (σ) measurements: PDLLA/CNC solution-cast composite films and electrospun fiber mats. The collection time for the electrospun fiber mat was 2 h; therefore, the sample thickness was controlled in a range of 100–300 μm. The thickness of the cast film was also controlled in a range of 300–600 μm. Both sample thicknesses were smaller than the gauge of the probe (1.5 mm). For samples with high conductivity ($\sigma > 10^{-6}$ S), the standard 4-point probe technique was applied to determine conductivity using a Keithley 2400 sourcemeter. For samples with low conductivity ($\sigma < 10^{-6}$ S), a Keithely 6487 electrometer, equipped with a Keithley 8009 resistivity testing fixture, was used following the ASTM D257 standard.

RESULTS AND DISCUSSION

Decreasing the solution concentration is a feasible way of producing thin fibers; however, only beaded fibers can be obtained when the solution concentration is reduced to a certain concentration (without sufficient high entanglement density). Previous studies have shown that the required minimum solution concentration for obtaining smooth and bead-free PDLLA fibers is 19 wt % for PDLLA (178k) solution electrospinning.[16] When filler was added to the prepared semidilute solution, the solution entanglement status and conductivity were both enhanced, which help eliminate the formation of beads; therefore, relatively smooth fibers can be obtained from these low-concentration solutions. The first part of this work investigates the effect of filler on the solution properties and as-spun fiber morphologies. The detailed experimental results are discussed below.

Role of Entanglement in Electrospinning Solution

Sufficient entanglement density in a given solution is an important requirement for obtaining electrospun products with fiber-like structures. In solutions with concentrations lower than the entanglement concentration, electrospinning eventually degenerates into electrospraying. Thus, determining the entanglement concentration (c_e), at which chain entanglement begins, is important. Theoretically, it can be determined from the log–log plot of the solution's specific viscosity versus the volume fraction of the polymer, as proposed by McKee et al.[5] It can also be determined using a theoretical calculation. When a solution concentration reaches c_e, sever chain overlapping occurs; at this concentration, the polymer volume fraction in the solution is defined as ϕ_p, the critical volume fraction. The ϕ_p can be estimated using classical relation $\phi_p = 2\ M_e/M_w$,[6] where M_w is the molecular weight and M_e is the entanglement molecular weight of the polymer, is used. After substituting the value of $M_w = 1.78 \times 10^5$ and $M_e = 5600$ g/mol into equation mentioned above, the calculated ϕ_p is about 6.3 % (corresponding to $c_e \sim 8$ wt %) for the PDLLA solution. Generally, during the electrospinning of polymer solution with a concentration of c, in the concentrated regime ($c > 2c_e$), electrospun products are all smooth fibers. When the solution concentration is in the semi-dilute entangled regime ($c_e < c < 2c_e$), electrospun products with a beaded-fiber shape are obtained. In the dilute regime ($c < c_e$), only beads are obtained during electrospinning.[5,6,16] For completely stable fiber formation during the PDLLA solution electrospinning process, a 19 wt % solution concentration at $\sim 2.4\ c_e$ is required. The experimental results are fairly consistent with the prediction.[6] Therefore, for a 13 wt % PDLLA solution (without sufficient entanglement density), only beaded-fibers are obtained during electrospinning.

According to this analysis, the status of the solution chain entanglement plays a very important role in determining the morphology of electrospun products. We speculate that a new network is generated between the PDLLA chains and the CNC particles when CNCs are added to the solution. When the polymer chains wrap the CNC filler, the polymer chain entanglement status in the solution is enhanced. However, determining the density of the entanglement in solutions with filler is difficult. Thus, the PDLLA/CNC solution rheology is investigated to determine if a new network forms between the PDLLA chains and the CNC particles.

Effect of CNC Filler on Solution Properties

To investigate the CNC concentration effect on solution properties, various amounts of CNC filler, ranging from 0 to 5 wt %, were added to 13 wt % PDLLA solutions. Figure 1 shows a log–log plot of G', together with η^*, versus ω of the PDLLA/CNC solutions. The figure indicates that, as a result of the addition of CNCs (i.e., 1, 3, and 5 wt %) to 13 wt % PDLLA solutions, the value of G' increased at low frequencies in the oscillatory shear mode rheology experiment. At a slope of 1.98, the solutions without filler exhibited a homogenous status. In contrast, an increasing G' was detected in the low-frequency regime, ca. $\sim$10 times larger than that of solution without filler, when CNCs were added. The plateau modulus increased with increasing CNC content [Figure 1(a)]. A modulus plateau was clearly observed when the CNC content was increased to 5 wt %. The increasing G' and the formation of the modulus plateau indicate that the formation of a new network between the PDLLA chains and the CNC particles is plausible. The η^* value of PDLLA/CNC solution can be derived from the dynamic properties (G' and G''). The η^* value exhibited only a slight increase with the addition of 1 wt % CNCs to the solution. This indicates that the PDLLA/CNC composite solution exhibits Newtonian fluid behavior and remains in a homogenous state. When the CNC content was increased, the solution became a non-Newtonian fluid, and η^* decreased dramatically in high frequency regions in the oscillatory shear experiment. A yielding behavior was detected in the solution with 3 wt % (or higher) CNCs [Figure 1(b)]. This behavior became distinct when 5 wt % CNCs were added to the solution. This implies that the aggregation of CNCs might occur at this concentration.

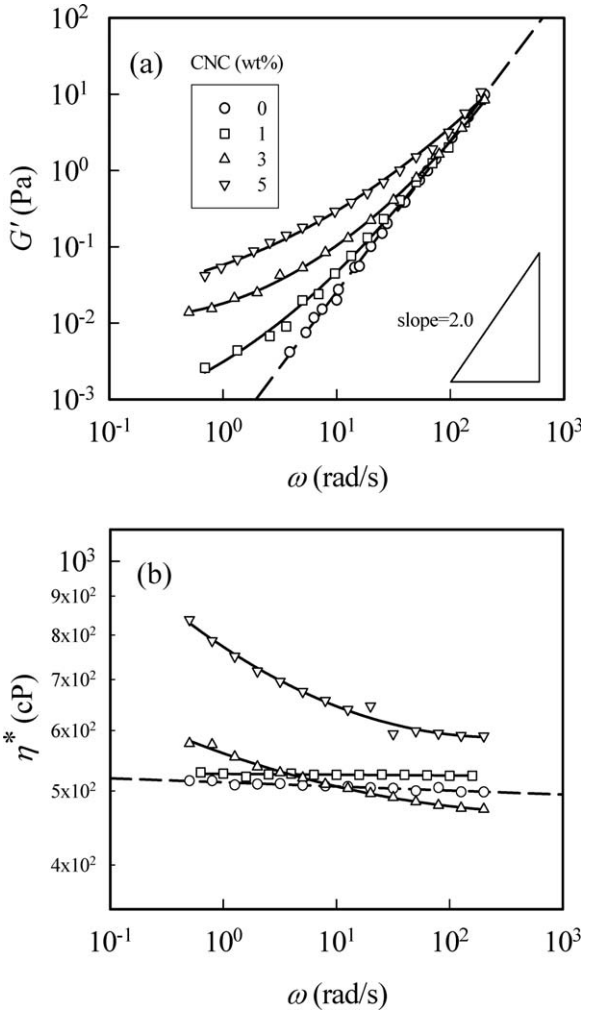

Figure 1. The viscoelastic properties of the PDLLA/CNC solutions. (a) the storage modulus G' (ω) of the 13 wt % PDLLA solutions filled with various amounts of CNC and (b) the corresponding complex viscosity, η^*.

Some studies have been conducted on particle-filled polymer solutions; the results frequently indicate an enhancement in viscosity (i.e., an increase in the zero shear viscosity of a solution with filler over that of a solution without filler).[17,18,36–38] Wang and coworkers[17] used TiO_2 as filler to investigate the effect of filler on the morphology of electrospun fiber. Menini and Farzaneh[18] reported that addition of PTFE particle enhanced the solution viscosity. Rayment et al.[39] revealed the effect of size and shape of particulate on the solution rheology. This behavior has also been found as CNT was added to the poly(methyl methacrylate)/DMF[37] and poly(vinylidene fluoride) (PVDF)/DMF solutions.[38] However, these studies only demonstrated the as-spun fiber morphology without explaining in detail the correlation between the filler and the entanglement state in solution.

As for other solution properties, after adding 1 wt % CNCs to 13 wt % solutions, κ was significantly increased by up to 15-fold compared to that of solutions without CNCs; the solution η^* value was also enhanced. In contrast, δ was remained unchanged. A similar trend was found in the 10 wt % solutions. The detailed effects of the addition of CNCs on the properties of PDLLA solutions are listed in Table I. The solution with filler was subjected to electrospinning to investigate the effect of filler on the morphology of electrospun fibers.

Effect of CNC Concentration on Electrospinning and As-Spun Fiber Morphology

We believe that the requisite entanglement density of a solution can be obtained either by increasing the polymer concentration or by introducing insoluble filler. Using this concept, 0–5 wt % (based on solution weight) CNC filler was added to 13 wt % solutions to prepare electrospun PDLLA/CNC composite fibers. According to the results of rheology experiment, the entanglement status in the solution can be enhanced by adding CNC filler. The addition of CNC particles not only changed the solution properties of PDLLA/DMF, however, but also significantly altered the functioning domain for electrospinning. Figure 2 shows the functioning domain for electrospinning 13 wt % PDLLA solutions with various CNC loadings. In general, for a fixed flow rate (Q), a higher applied voltage (V) is required for electrospinning solutions with higher conductivity. As demonstrated in the reported literature, a scaling law of $(V/H) \sim Q^{\alpha}$ was established to describe the electrostatic field required for a stable cone-jet electrospinning mode.[36] The derived exponent α in this experiment is in the range of 0.08–0.20 for the solutions with different amounts of CNC filler. The nominal electric field required is the largest for the solution with 5 wt % CNCs due to its high solution conductivity. The obtained results consist with the previous findings. A common operation window for fixing the Q-V variables to determine the effect of filler is not available because of the enhanced solution conductivity. This phenomenon has been observed during the electrospinning of PS/DMF solutions to which salt was added.[9] Thus, the required V for each solution was chosen as 1/2 (V_{us}-V_s), where V_{us} and V_s are the upper and lower bound voltage required for the stable cone-jet mold electrospinning.

Figure 3 shows the SEM and TEM images of the fibers collected from electrospinning 13 wt % solutions with various amounts of CNC filler under conditions of $Q = 0.3$ mL/h, $H = 7$ cm, and V values ranging from 7.5 to 11.0 kV (based on Figure 2). To faithfully present the genuine fiber morphology, SEM images with a low magnification were preferred rather than using the

Table I. Effect of CNC Content on the Solution Properties and the As-Spun Fiber Diameter

PDLLA (wt %)	CNC (wt %)	κ (μS/cm)	γ (dyne/cm)	D (nm)	d_f (nm)
13	0	6.4	36.3	1280 ± 480	70 ± 13
	1	97.2	35.9	150 ± 45	85 ± 10
	3	101.4	36.2	195 ± 55	83 ± 13
	5	115.4	35.4	354 ± 77	98 ± 15
10	0	6.5	35.9	1450 ± 940	60 ± 10
	1	99.1	35.5	1170 ± 540	85 ± 15

D and d_f are the diameter of bead (or CNC aggregation) and the fiber portion, respectively.

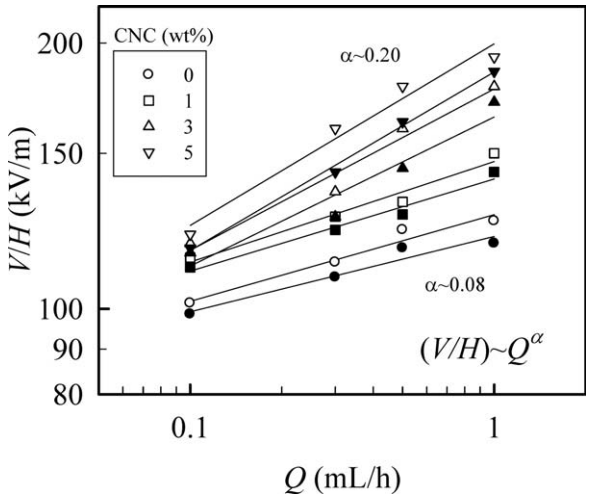

Figure 2. Functioning domain for electrospinning of the 13 wt % PDLLA solutions with different CNC loadings, which indicates the range of operating voltages required for the stable cone-jet mode electrospinning. (Filled and open symbols denote the lower and upper bound electric field, respectively. $H = 7$ cm.)

high magnification images, which may lead to misleading interpretation. On the other hand, the aggregation of CNCs could be readily detected by TEM images with a high magnification, as shown by the inset. According to the TEM observation, the primary particle size of the CNCs is about 40 nm. Without the addition of CNCs, only beaded fibers were produced during the 13 wt % solution electrospinning, as mentioned previously. The inset shows the enlarge portion of electrospun fiber to reveal the difference in beaded fibers. Spindle-like beads along the fiber strings could be clearly observed in the SEM image [the inset of Figure 3(a)], whereas higher magnification image of CNC particles [Figure 3(b)] was also demonstrated. The addition of 1 wt % CNCs led to a pronounced reduction in bead formation [Figure 3(c)]. Under a higher SEM magnification, the irregular structures along the PDLLA fibers were different from the spindle-like beads produced from CNC-free solutions [inset of Figure 3(c)]. The TEM images clearly demonstrate that the slightly protruding portion from the smooth fiber is due to the presence of CNC particles [Figure 3(d)]. The obtained PDLLA/CNC composite fiber diameter is about 90 nm.

With increasing amount of CNC filler added to the solution, several CNC particles aggregated during electrospinning and formed an irregular structure along the fibers. As shown in Figure 3(e), the aggregation of CNC particles became more distinct when the CNC content was increased to 5 wt %, which corresponds to ~23 vol % CNCs distributed in the solvent-free PDLLA fibers. The as-spun PDLLA/CNC fiber diameters were smaller than those of the CNC aggregates. Thus, the protrusion of these aggregates from the fiber surface, with an appearance similar to the beaded fibers, was inevitable. Upon further inspection using TEM, most of the observed bead portions were found to have been formed by the aggregation of CNC particles [Figure 3(f)]. This observation is consistent with the rheological results of solutions with filler, where CNC aggregation was observed in the solution with higher CNC loadings. Therefore, an appropriate CNC content (1 wt % in our study) in the prepared solution is required to produce smooth electrospun fibers.

The addition of 1 wt % CNCs into 13 wt % PDLLA solution led to a pronounced reduction in bead formation. A solution with 10 wt % PDLLA concentration, which is the margin concentration of the semidiluted regime (c is a little higher than c_e), was used to further investigate the effects of filler on electrospun product morphology. CNCs (1 wt %) were added to 10 wt % PDLLA solutions, which were then subjected to electrospinning. When the 10 wt % PDLLA solutions were electrospun, most of the products were beads and little fibers were obtained, indicating that the polymer chain entangled network was not strong enough to prevent the formation of beads. Some fibers (not only beads) were obtained during electrospinning as a result of adding 1 wt % CNCs to the 10 wt % PDLLA solution (Figure 4).

The addition of filler enhanced the entanglement status in the solution, leading to more electrospun products having a fiber shape. However, as more CNCs were added into the solution, the number of beads did not decrease significantly. This implies that an appropriate polymer concentration is required to maintain the basic entanglement strength in the solution to avoid bead formation. The diameter of PDLLA/CNC composite fibers is larger than that of pure PDLL fibers. CNC particles may act as an anchor, during the fiber formation stage, to entangle with the polymer chains. In conclusion, the addition of CNC filler provided an extra network between the polymer and CNCs to reduce the formation of beads; however, the additional network structures did not completely take place the role of polymer–polymer chain entanglements.

Proposed Additional Network in the Ternary System of PDLLA/DMF/CNC

According to the results of rheology experiment, we know that the additional network formed coexists with the original PDLLA-PDLLA chain network in the ternary system of PDLLA/DMF/CNC. The formation of an additional network promotes the chain entanglement status and strengthens the solution deformability to prevent beaded fiber formation during electrospinning as mention above. When CNCs are added to the PDLLA solution, two possible additional network structures might develop besides polymer chain entanglements. They are PDLLA-CNC and CNC-CNC networks. Because of their low aspect ratio, CNCs do not easily form a CNC-CNC network like that of CNT filler disperse in polymer solution.[40] Therefore, we speculate that most of the additional network was the PDLLA-CNC network, as shown in Figure 5. We hypothesis that the individual polymer chains between CNCs act as bridges by wrapping the CNCs at both chain ends to form a polymer-CNC hybrid network. To form such a network, a single polymer chain must be long enough to wrap the CNC particle at least once with enough of the polymer chain left over to form a random coil in between CNC particles. The monomer units required to effectively wrap CNCs depend on the size of CNCs and the polymer-CNC bonding.

Applied Polymer SCIENCE

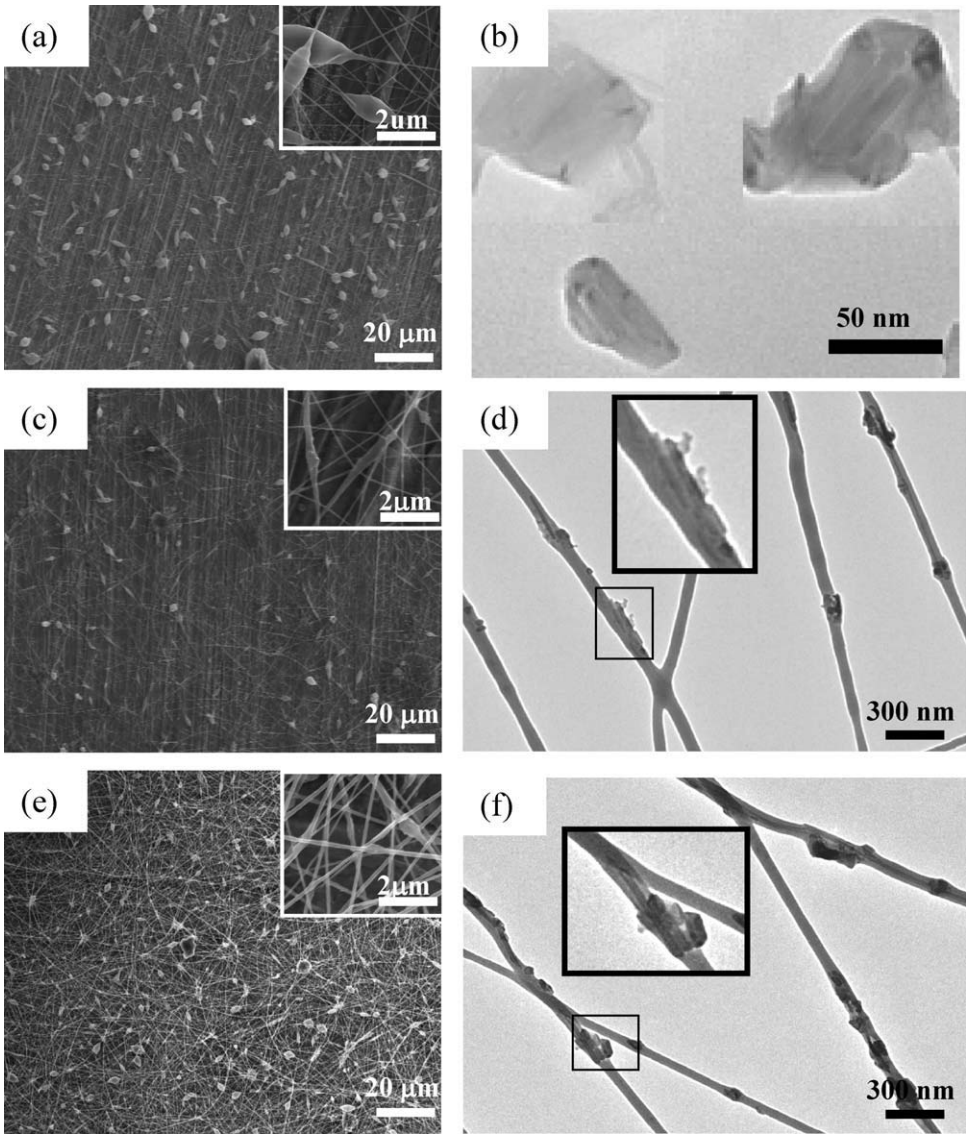

Figure 3. Electron microscope images of electrospun fiber mat obtained from the 13 wt % PDLLA solution with various CNC loadings. (a) SEM image of electrospun fibers obtaining from as-prepared solution without the addition of CNCs, (b) TEM image of CNC particles, (c) SEM, (d) TEM image of electrospun fibers with 1 wt % CNC loadings, (e) SEM, and (f) TEM image of electrospun fibers with 5 wt % CNC loadings. The inset shows a higher magnification of the selected area (0.3 mL/h, $H = 7$ cm, 7.5–11.0 kV).

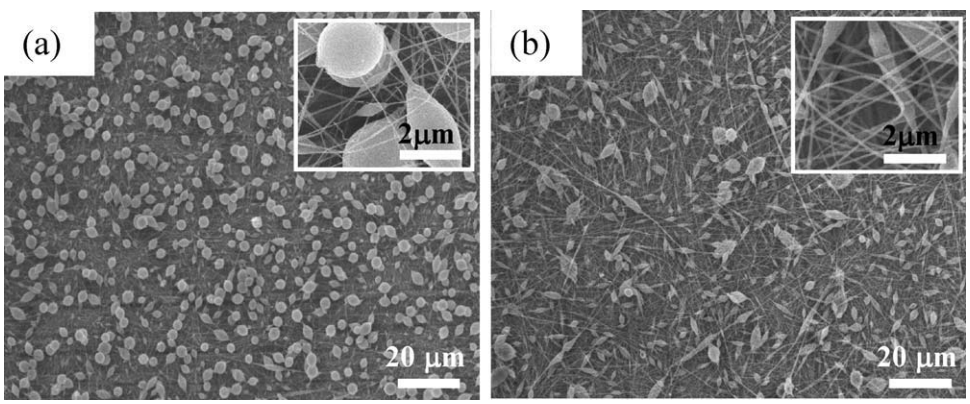

Figure 4. SEM images of electrospun product prepared from 10 wt % PDLLA solution (a) without and (b) with 1 wt % CNC. (The inset shows the enlarge portion of beaded fibers.)

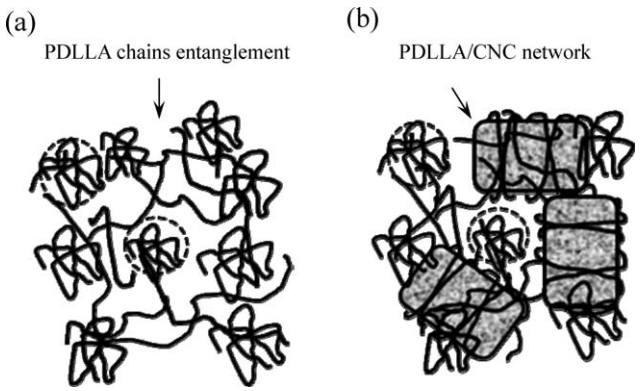

Figure 5. The carton of the PDLLA chains entangled with CNC particles. (a) Illustration of interaction of PDLLA chains and (b) additional network formation between polymer chains and CNCs in solution state (the circled part indicates a portion of a random coil).

The length of a fully extended PDLLA chain (r) can be simply determined by taking the product of monomer length and the number of monomers in a polymer chain. The length of a monomer can be estimated by choosing $n_v = 6$ and $l_v = 1.4$ Å, where n_v and l_v are the number of real or virtual bonds per monomer repeat unit and the length of such a bond, respectively. The molecular weight of the monomer was measured to be 144 g/mol.[41] The estimated length of the fully extended PDLLA chains is about ~ 1040 nm. Compared to the CNCs average particle size (~ 40 nm), a CNC (aspect ratio ~ 2) has a circumference of 125–250 nm. Basically, the length of PDLLA chain is sufficiently long to wrap a CNC particle. The random coil size can be estimated using the following equation: $6\langle R_g^2\rangle/M_w = \langle R_o^2\rangle/M_w$, where $\langle R_g\rangle$ and $\langle R_o\rangle$ are the radius of gyration and the root-mean-square end-to-end distance of the polymer chain, respectively. A $\langle R_o^2\rangle/M_w$ of 0.699 Å^2 mol g^{-1} was reported for a PDLLA (28% D-form) by Anderson and Hillmyer.[38] For a given M_w, the calculated average diameter of random coils for the present PDLLA, $\langle R_g\rangle$, is 14.4 nm. It should be noted that this value was theoretically estimated under a theta solvent condition. The radius of gyration of PDLLA should be larger in the PDLLA/DMF solution as DMF is commonly regarded as a good solvent for PDLLA. Based on the argument, in the solution state, PDLLA chains can wrap CNCs, acting as bridges between CNCs. The remaining chain segments between the grasped CNCs are still long enough and likely to entangle to each others, provided that the long chain nature is still preserved, as shown in Figure 5. Based on the above discussion, the polymer chain would be long enough to wrap the CNC particles to form the network structure between the polymer chains and CNC particles. A similar concept was used to describe the entangled status of PS/CNT composites.[42]

We demonstrated that the addition of CNC filler can produce more entanglements between the polymer chains and the CNCs in a given solution. The addition of an extra network enhanced the entanglement status in the solution, leading to electrospun products having a relatively smooth fiber shape. The thinnest obtained smooth PDLLA/CNC composite fiber diameter (~90 nm) is smaller than the PDLLA/CNT composite fiber diameter (~560 nm) reported in the literature.[28] To our knowledge, this is the smallest smooth PDLLA composite fiber ever reported. The effect of filler becomes more significant for filler with a larger aspect ratio (i.e., 20 times larger than that of CNC), such as CNTs. More studies are being performed in our laboratory to investigate the effect of aspect ratio on the rheological properties of a solution. Results will be published in a future article.

Characterization of Electrospun PDLLA/CNC Composite Fiber

In our previous study, the finest PDLLA electrospun fiber ($d_f \sim$ 350 nm) was produced via a high temperature electrospinning process.[16] In this study, we further reduced the electrospun composite fiber diameter to less than 100 nm by introducing filler into the semidilute solution for electrospinning. For such a narrow fiber diameter, investigating the effect of filler on the microstructure of the composite fiber is of interest.

WAXD was used to inspect the effect of CNC filler on the crystal modification of PDLLA/CNC composite fibers (Figure 6). For electrospun fiber mats without CNC filler, only a broad amorphous halo was observed in the WAXD profile (Figure 6, curve-a), indicating that the as-spun PDLLA fiber mats were amorphous. In the WAXD diffraction profile for the CNC particle materials without a polymer, an broad peak at around 2θ = 23.0–27.0° was observed. The peak center position is about $2\theta = 26.2°$, which is caused by the diffraction of the layer structure of the CNCs (interlay spacing of the shell layers is about 0.34 nm), which is close to that of the graphite (002) plane.[21] For electrospun fiber mats containing CNC filler, a halo and two peaks at around 2θ =24.3 and 26.2° were observed (Figure 6, curve-b).

We speculate that the extra peak at $2\theta = 24.3°$ might have resulted from the CNC particles, as no such peak was found in the as-spun PDLLA fiber mats, or an induced polymer crystal structure forming outside the CNC particles when the PDLLA/

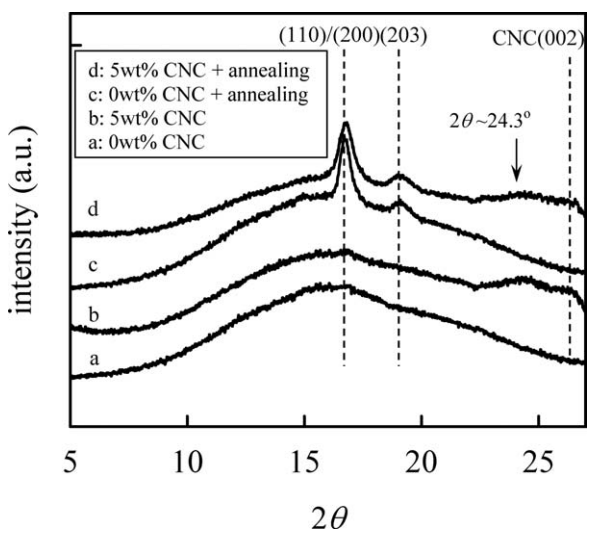

Figure 6. WAXD intensity profiles of electrospun PDLLA/CNC composite fibers before and after annealing. The electrospun fibers were obtained from the 13 wt % PDLLA solution with 0 and 5 wt % CNC loadings. (Annealing process: fiber mats are annealed at 91°C for 5 min.)

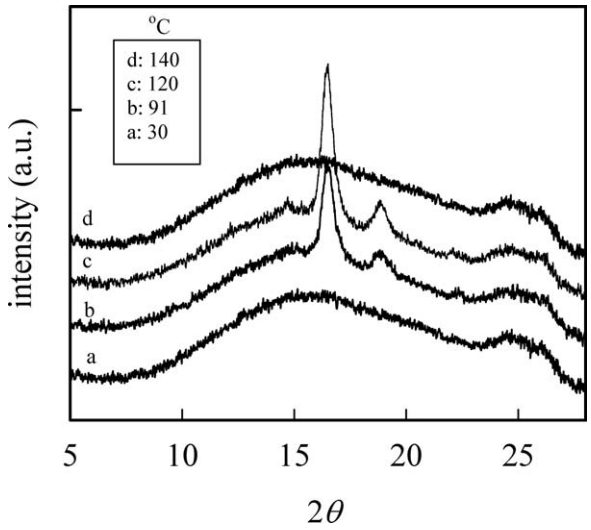

Figure 7. A stepwise heating WAXD intensity profiles of PDLLA/CNC composite fibers, the electrospun fibers were obtained from 13 wt % PDLLA solution with 5 wt % CNC loadings. (Isothermal process: fiber mats are annealed at each temperature for 10 min.)

CNC solution was electrospun into fibers, or both. Inoue and coworkers[43] found that the peak at $2\theta = 24.6°$ appears when the PLLA was annealed at a lower crystallized temperature (<110°C). They indicated that this regular structure is the α′-form crystal. Zhang et al.[44] indicated that both the α′- and α-form crystals have the same 10_3 helix chain conformation and orthorhombic unit cell. However, the packing of the side groups in the helical chains of the α′-form crystal is less ordered and looser than that of the α-form crystal. It should be noted that although our PDLLA/CNC electrospun fibers did not undergo any heat treatment, this unique peak was still observed in the WAXD profiles.

To clarify the origin of this peak ($2\theta = 24.3°$), a sample was first annealed at 91 °C for 5 min to conduct the crystallization process, as reported in a previous study.[16] The obtained results show that the PDLLA polymer crystallized after the annealing process; two major diffraction peaks, at $2\theta = 16.5°$ (110/200) and 18.9° (203), formed. These diffraction peaks resulted from α-form crystal modification (Figure 6, curve-c).[43,44] Compared to the obtained WAXD profiles of the annealed electrospun PDLLA fiber mat, only the α-form crystal was detected in both the PDLLA and composite fibers after annealing. Therefore, the PDLLA crystal was thus not significantly altered by the addition of CNC filler. However, the peak at $2\theta = 24.3°$ was not significantly altered as the PDLLA/CNC composite fibers conducted a heat treatment (Figure 6, curve-d). An *in situ* WAXD detection was conducted on the PDLLA/CNC composite mat during a stepwise heating procedure (steps of 10°C from 91 to 150°C). The peak at $2\theta = 24.3°$ still existed when the PDLLA/CNC composite sample melted (Figure 7). Thus, we confirmed that the peak at $2\theta = 24.3°$ was not resulting from the polymer itself. During the manufacture of CNC particles, a small amount of CNT might coexist with the desired CNCs. These traced CNTs are occasionally seen in the as-spun PDLLA/CNC fibers (Figure 3), giving rise to the small reflection peak at $2\theta \sim 24.3°$ in the WAXD pattern. A similar WAXD peak was also reported by Yu et al.[45]

Figure 8 shows the heating traces of electrospun fiber mats with various amounts of CNC filler. The as-received pellets showed no clear cold crystallization or melting peaks during heating at a rate of 10°C/min. Upon annealing at 91°C for 24 h, the slow-crystallizing species finally developed a small crystallinity percentage of 6.5% with a single melting peak at 117.4°C (not shown for brevity). In contrast, the first heating trace of the as-spun PDLLA fibers showed a small cold crystallization peak at 101.2°C, followed by a melting peak at 124.9°C (Figure 8, curve-a). The second heating trace only showed a small enthalpy recovery peak around the glass transition temperature (T_g) in the absence of crystallization and melting events (not shown here). This indicates that the crystallization behavior of the PDLLA polymer was enhanced when the PDLLA was electrospun into a fiber shape. We believe that a polymer chain orientation developed during jet stretching in bending instability region, leading to a fast crystallization route during heating.[2,46]

The samples containing CNC filler clearly showed exothermic peaks that could be correlated with the crystallization of PDLLA fiber mats; the corresponding temperature is denoted as T_c. For the fiber containing CNC filler, the measured T_c shifted to a lower temperature. The T_c dose strongly depended on the loading of CNC filler in the fiber mat and the normalized crystallization enthalpy ($\Delta H_c'$) increased with increasing CNC content (Table II). According to the cooling trace of the PDLLA/CNC composite mats after the first heating run, the crystallization exothermic peak was not observed. This implies that CNC filler might not be a good nuclear agent for a slow crystallized PDLLA polymer. Thus, we believe that because CNCs are a good conductor of heat, the oriented polymer chain packed and crystallized more easily around the CNCs during heating. The cause of the enhanced crystallization behavior was different to

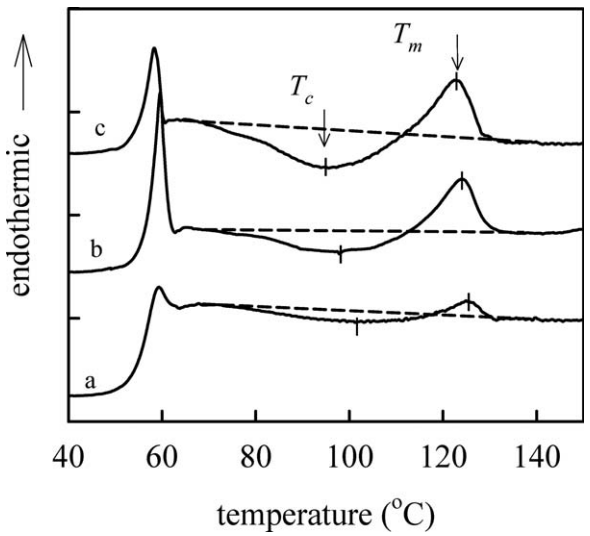

Figure 8. DSC heating traces of electrospun fibers with different CNC loadings; electrospun fibers were obtained from the 13 wt % PDLLA solution containing 0 (curve-a), 1 (curve-b), and 5 (curve-c) wt % CNC.

Table II. Thermal Properties of Fibers Electrospun from the 13 wt % PDLLA Solution Containing Different Amounts of CNC

CNC (wt %)	T_g (°C)	$\Delta H_r'$ [a] (J/g)	T_c (°C)	$\Delta H_c'$ [a] (J/g)	T_m (°C)	$\Delta H_m'$ [a] (J/g)	X_c [b] (%)
0	56.8	0.31	101.2	1.07	124.9	0.85	0.9
1	55.3	2.18	97.5	2.99	124.0	2.96	3.2
3	55.0	2.19	95.7	3.98	123.2	3.88	4.1
5	54.5	2.09	93.9	5.23	122.5	4.94	5.3

[a]Normalized with weight fraction of PDLLA component, [b]X_c is calculated using the equation of $\Delta H_m'/\Delta H_f$, where ΔH_f is the heat of fusion for a 100% PDLLA crystal.

that of CNTs embedded in a PLLA polymer since CNTs are regarded as an effective nucleating agent.[47]

As the fiber containing more CNCs filler, the measured melting temperature decreased to 122.5°C during the heating scan (Figure 8, curve-c). As confirmed by the WAXD patterns, a lower melting temperature did not result from the changing of PDLLA crystal modification. The normalized heat of fusion ($\Delta H_m'$) of the PDLLA/CNC electrospun fibers increased with increasing CNC content (Table II). This indicates that the PDLLA polymers crystallized more easily during heating as CNC is a good conductor of heat. Therefore, a thinner lamellar was formed due to the fast crystal growth rate, leading to a relatively low-melting temperature during the heating scan. Enthalpy relaxation behavior was found at around T_g and became more distinct as the CNC filler was added to the fibers. This suggests that the free volume of PDLLA chains in the as-spun composite fibers was significantly reduced. The normalized loss of enthalpy ($\Delta H_r'$, ca. $\sim$ 2.0 J/g) associated with the free volume reduction was recovered as an endothermic (aging) peak in the glass transition region. The detailed thermal properties are listed in Table II.

Electrical Conductivity of Electrospun PDLLA/CNC Composite Fiber Mat

The conductivity of the electrospun fiber composite mat was determined using the four-point probe measurement method.[29,48–53] As described in the literature, when the sample thickness is less than the probe spacing, the resistivity (ρ) can be calculated using: $\rho = K\,(V/I)$, where V and I are the potential applied across the probes and the measured current, respectively. And the value of K is closely related to the sample thickness and testing fixture.[54] The sample conductivity (σ) is simply the reciprocal of ρ : $\sigma = 1/\rho$. The obtained conductivity of the electrospun fiber mat is the volume conductivity in units of S cm^{-1}.[29,48–52] Gorga and coworkers[26] used flat interdigitated electrodes combined with a handmade testing fixture to carry out the electrical measurements. Their obtained conductivity of an electrospun fiber mat was the surface conductivity in units of S. Ounaies et al.[51] reported that for a conducting composite the obtained surface conductivity showed a similar behavior to the volume conductivity, with an overall lower conductivity.

The conductivity of the PDLLA/CNC composites, with respect to the filler concentration, is shown in Figure 9. Two alternative samples were prepared to study the electrical conduction behavior. One is a solution-cast film that ignores the void space, minimizing the effects of the mat morphology, and the other is a porous electrospun fiber mat. The measured conductivity of the as-spun PDLLA fiber mat is about 1.6×10^{-17} S cm^{-1} in a nonconducting state. A sharp increase in the conductivity was observed for filler content of 0.23–0.27 volume fractions [Figure 9(a), curve-a]. When the filler content of the fiber mats was above a 0.27 volume fraction, the conductivity changed moderately. This behavior is indicative of a percolation transition. The percolation threshold of the PDLLA/CNC composite fiber mat is between 0.23 and 0.27 volume fractions. Compared to the

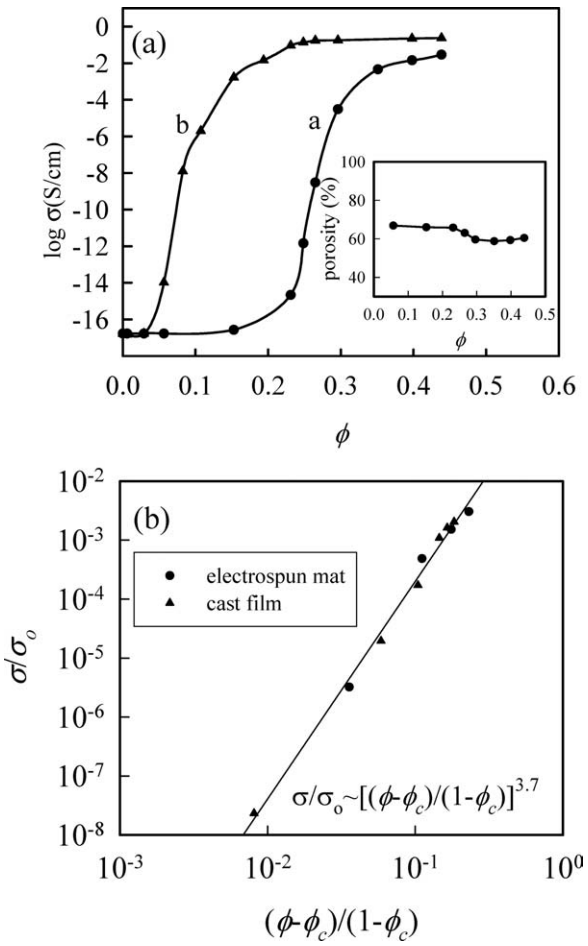

Figure 9. The electrical properties of PDLLA/CNC composite fiber mat and cast film. (a) Conductivity curves of PDLLA/CNC electrospun fibers (curve-a) and cast film (curve-b), the inset shows the porosity of electrospun fiber mat; (b) the master curve of the conductivity of PDLLA/CNC system.

reported percolation threshold of CNT in PS electrospun mats is around 4 wt %.[25] For MWNT in PEO nanofibers mat, the percolation threshold ranges from 0.25 to 0.50 wt %.[26] For MWNT in single and coaxial bicomponent PEO fibers, the percolation threshold concentrations are 0.45 and 0.015 wt %, respectively.[27] For the PLA/MWNT fiber mat, the percolation threshold is 0.30 wt %.[28] We considered that this large gap is a result of the morphology differences of the additive fillers, since the CNC can regard as granule particles.

For further comparison, the conductivity of a PDLLA/CNC solution-cast film was also measured [Figure 9(a), curve-b)]. The conductivity of the electrospun composite mats versus the CNC concentration curves can be further characterized by the classical percolation theory.[53] According to the theory of transport in isotropic percolating materials, the conductivity data above the percolation threshold can be fitted and described using the following equation: $\sigma \sim (\phi - \phi_c)^t$ for $\phi > \phi_c$, where ϕ is the volume fraction of the conducting filler in the composite, ϕ_c is the critical volume fraction (volume fraction at percolation), and t is a critical exponent. In general, this equation can be used to describe the conduction behavior of composites; some researchers have also used this equation to describe the conduction behavior of a deformable fiber mat. The characteristics of the sample morphology (e.g., cast film and electrospun fiber mats) may strongly influence the nature of the percolation process and the conductivity of the prepared sample.

The obtained critical CNC volume fractions for the cast film and electrospun fiber mats were 0.10 ± 0.01 and 0.26 ± 0.01, respectively. As expected, the obtained conduction curves of the cast film and fiber mats were different. The difference of conductivity between cast films and electrospun fiber mats has also been observed for polyaniline/PEO blends.[48] We believe that this large gap is a result of the morphology differences of the samples. Electrospun fiber mats are highly porous and contain many voids filled with insulating air. In contrast, dense films with a high density are obtained from the solution casting approach.

In a composite, electron transport is governed by electron tunneling through insulation materials (i.e., PDLLA), separating two neighboring conducting materials (i.e., CNC). Comparing the morphology of the PDLLA/CNC cast film with that of the electrospun fiber mats, there is an extra phase in the fiber mats, that is, void space (or air space). A cast film is similar to a bulk composite sheet; there is no insulating void space inside the bulk sample to separate the two conducting parts. Therefore, a relatively low percolation threshold was observed in the cast film. We speculate that in the extreme case of no void space inside the fiber mat, the conduction behavior would be similar to that of bulk composites. Therefore, the effect of the porosity of electrospun fiber mats was investigated in the next.

The porosity of electrospun PDLLA/CNC fiber mats was measured using the equation $(1 - P/P_o) \times 100\%$, where P is the density of electrospun composite membranes, and P_o is the density of bulk composites.[55] The density of the bulk composites was calculated by assuming that the volume of the composite can be added, as PDLLA and CNC are deemed immiscible. The obtained porosity of the electrospun fiber mats was in the range of 60–65% [inset of Figure 9(a)]. It should be noted that obtained porosity of the mat may differ with the electrospun fiber morphology.[16,50,55] According to the experimental results, the conductivity of the electrospun PDLLA/CNC fiber mat was closely correlated with the solid content in the mat. Because of the high porosity, the fiber mat contained many voids filled with air. To provide a similar conducting path for CNC contacts, a higher CNC content was required in the fiber mat than in the cast film.

Therefore, the real volume fraction of the composite fiber mat was normalized by multiplying it by the solid content (0.40–0.35) of the fiber mat. The normalized conduction curve eventually overlaps with the conduction curve of the cast film (figure not shown). This finding indicates that the conducting behavior in both samples is similar. When the electrospun fiber mat was hot pressed to become a solid film, the measured conductance of film was similar to the cast film.

In conclusion, provided that the porosity was taken into account, the conduction behavior of the fiber mat became similar to that of bulk composites. After normalized with the solid content, the threshold concentration for the fiber mat is similar to that of the cast film (~ 0.1). To our knowledge, only a few studies take this porosity effect into an account on the conduction behavior of the mat, Laforgue and Robitaille[50] normalized their obtained conductivity of the mat with porosity to evaluate individual fibers conductivities.

Conduction Behavior of Electrospun PDLLA/CNC Composite Fiber Mat

When the ϕ_c values of the cast film and as-spun fiber mat were determined, the corresponding t values were also obtained. In this study, the obtained t values are 3.1 ± 0.6 and 3.2 ± 0.8 for the PDLLA/CNC solution cast films and electrospun fiber mats, respectively. The derived t values in our experiment also agree with the predicted value of 3.0 obtained using the mean field model.[56] Although a universal value of $t = 2$ is proposed by the numerical calculation of the random-resistor models for three-dimensional lattices,[57] almost 50% of the measured critical exponents deviate from this value, depending on the added filler type.[58] The t values obtained in this study were somewhat larger than the universal value of 2, indicating that the tunneling conduction behavior of the samples led to nonuniversal values.[58–60] On the other hand, in PDLLA/CNC composites, the obtained value of t was consistent with experiments conducted using a granular metal, RuO_2, embedded in an insulating glass matrix (t =2.15–3.84)[58] because CNCs with a low aspect ratio can be regarded as conducting particles.

Based on the effective medium theory,[56,61–62] when the CNC content increased to above the critical percolation concentration, a modified scaling law is proposed to describe the σ value above the percolation threshold: $\sigma_o[(\phi - \phi_c)/(1 - \phi_c)]^s$, where σ_o is the intrinsic conductivity of the filler, and the term in the bracket refers to the level of the percolation network. After a careful regression analysis, the log–log plot of σ/σ_o versus $(\phi - \phi_c)/(1 - \phi_c)$ is shown in Figure 9(b). A master curve obtained in the conduction regime indicates that the composite

cast film and the electrospun fiber mat exhibited similar conduction behavior when the CNC content was above the critical percolation concentration. The derived σ_o is about 1.0 S cm^{-1}, indicating that CNC is a conducting material. However, we also observed that the intrinsic conductivity of the CNC filler in the composite of PS/CNC is about 5.8×10^{-4} S cm^{-1}.[63] The difference in electrical conductivity obtained between these two systems is plausibly attributed to the different preparation methods for the composites; compression molding was used for the PS/CNC film,[63] whereas solution casting was applied for the present PDLLA/CNC film. Moreover, the CNC raw material was treated with acid aqueous solution (H_2SO_4/HNO_3 = 3/1) to dissolve the impurities. After this process, CNCs may have some carboxyl groups on its surface. The polarities of PDLLA and PS are quite different. It eventually leads to different CNC dispersion in the prepared composites, thereby altering the electrical conductivity of the as-prepared composites. In the last, the obtained *s* value of the master curve is about 3.7, implying that the tunneling effect could be observed both in the cast film and in the deformable electrospun fiber mat.

CONCLUSIONS

We proposed and demonstrated that the addition of CNC to a semidilute solution caused the formation of a plausible new network between the polymer chains and filler particles, leading to an enhanced solution entanglement density. This was confirmed by the results of the oscillatory shear mode rheology experiment. The solution conductivity was also enhanced. These properties suppressed the formation of beads during electrospinning. We proved that the desired entanglement intensity for producing relatively smooth electrospun fiber could be achieved by adding filler to the semidilute solution. This method can be applied to produce ultra thin composite fibers. According to the WAXD profiles, the polymer crystal modification was not significantly affected by the addition of CNC filler. The DSC heating scan results show that the crystallization behavior was enhanced when the PDLLA was electrospun into a fiber shape. With CNC filler, the crystallization rate of the PDLLA matrix was further enhanced. However, the fast crystallization process leads to a thinner lamellar structure, resulting in a low-melting temperature.

The sample morphological characteristics, such as those of cast film and an electrospun fiber mat, strongly influenced the nature of the percolation process and the conductivity of the prepared sample. We examined the difference in the conduction behavior between the composite film and the deformable electrospun fiber mat. The results show that there is a close relationship between the two types of sample. When the porous effect of the electrospun fiber mat was eliminated, the conductivity curves of the mat and the cast film almost overlapped. Since the conductivity was characterized using classical percolation theory, the presence of tunneling conduction led to nonuniversal values of *t*. When the CNC content of the sample was increased to above the critical percolation concentration, in the conduction regime, a master curve was obtained as the conductivity curves were normalized with the level of the percolation network, $(\phi-\phi_c)/(1-\phi_c)$.

This article discussed in detail the effect of filler on solution properties, the electrospinning process, and as-spun fiber morphology. The obtained composite fiber microstructure was characterized and the electrical conduction behavior of the electrospun fiber mat was investigated.

ACKNOWLEDGMENTS

The authors are grateful to the Taiwan Textile Research Institute (ROC) for the research grant (Innovation Project-100142) that supported this work. They also thank Dr. G. L. Hwang in ITRI for providing the CNC fillers.

REFERENCES

1. Tan, S. H.; Inai, R.; Kotaki, M.; Ramakrishna, S. *Polymer* **2005,** *46*, 6218.
2. Zong, X.; Kim, K.; Fang, D.; Ran, S.; Hsiao, B. S.; Chu, B. *Polymer* **2002,** *43*, 4403.
3. Zhou, F. L.; Gong, R. H.; Porat, I. *Polym. Eng. Sci.* **2009,** *49*, 2475.
4. Wang, X.; Niu, H.; Lin, T. *Polym. Eng. Sci.* **2009,** *49*, 1582.
5. McKee, M. G.; Wilkes, G. L.; Colby, R. H.; Long, T. E. *Marcomolecules* **2004,** *37*, 1760.
6. Shenoy, S. L.; Bates, W. D.; Frisch, H. L.; Wnek, G. E. *Polymer* **2005,** *46*, 3372.
7. Gupta, P.; Elkins, C.; Long, T. E.; Wilkes, G. L. *Polymer* **2005,** *46*, 4799.
8. Bhattarai, S. R.; Bhattarai, N.; Yi, H. K.; Hwang, P. H.; Cha, D. I.; Kim, H. Y. *Biomaterials* **2004,** *25*, 2595.
9. Wang, C.; Hsu, C. H.; Lin, H. J. *Marcomolecules* **2006,** *39*, 7662.
10. Huang, C.; Chen, S.; Lai, C.; Reneker, D. H.; Qiu, H.; Ye, Y.; Hou, H. *Nanotechnology* **2006,** *17*, 1558.
11. Lin, K.; Chua, K. N.; Christopherson, G. T.; Lim, S.; Mao, H. Q. *Polymer* **2007,** *48*, 6384.
12. Liu, Y.; He, J. H.; Yu, J. Y.; Zeng, H. M. *Polym. Int.* **2008,** *57*, 632.
13. Givens, S. R.; Gardner, K. H.; Rabolt, J. F.; Chase, D. B. *Macromolecules* **2007,** *40*, 608.
14. Wang, C.; Chien, H. S.; Hsu, C. H.; Wang, Y. C.; Wang, C. T.; Lu, H. A. *Macromolecules* **2007,** *40*, 7973.
15. Zhou, H.; Green, T. B.; Joo, Y. L. *Polymer* **2006,** *47*, 7497.
16. Wang, C.; Chien, H. S.; Yan, K. W.; Hung, C. L.; Hung, K. L.; Tsai, S. J.; Jhang, H. J. *Polymer* **2009,** *50*, 6100.
17. Drew, C.; Wang, X.; Samuelson, L. A.; Kumar, J. *Macromol. Sci. Part A* **2003,** *40*, 1415.
18. Menini, R.; Farzaneh, M. *Polym. Int.* **2008,** *57*, 77.
19. Iijima, S. *Nature* **1991,** *354*, 56.
20. Iijima, S.; Ichihashi, T. *Nature* **1993,** *363*, 603.
21. Xu, B.; Guo, J.; Wang, X.; Liu, X.; Ichinose, H. *Carbon* **2006,** *44*, 2631.
22. Spitalsky, Z.; Tasis, D.; Papagelis, K.; Galiotis, C. *Prog. Polym. Sci.* **2010,** *35*, 357.

23. Dror, Y.; Salalha, W.; Pyckhout-Hintzen, W.; Yarin, A.; Zussman, E.; Cohen, Y. *Progr. Colloid. Polym. Sci.* **2005,** *130*, 64.
24. Moniruzzaman, M.; Winey, K. I. *Macromolecules* **2006,** *39*, 5194.
25. Mazinani, S.; Ajji, A.; Dubois, C. *Polymer* **2009,** *50*, 3329.
26. McCullen, S. D.; Stevens, D. R.; Robert, W. A.; Ojha, S. S.; Clarke, L. I.; Gorga, R. E. *Macromolecules* **2007,** *40*, 997.
27. Ojha, S. S.; Stevens, D. R.; Stano, K.; Hoffman, T.; Clarke, L. I.; Gorga, R. E. *Macromolecules* **2008,** *41*, 2509.
28. McCullen, S. D.; Stano, K. L.; Stevens, D. R.; Roberts, W. A.; Monteiro-Riviere, N. A.; Clarke, L. I.; Gorga, R. E. *J. Appl. Polym. Sci.* **2007,** *105*, 1668.
29. Hwang, J.; Muth, J.; Ghosh, T. *J. Appl. Polym. Sci.* **2007,** *104*, 2410.
30. Lim, L.T.; Auras, R.; Rubino, M. *Prog. Polym. Sci.* **2008,** *33*, 820.
31. Donald, G. *J. Polym. Environ.* **2002,** *9*, 63.
32. Kim, K.; Yu, M.; Zong, X.; Chiu, J.; Fang, D.; Seo, Y. S.; Hsiao, B. S.; Chu, B.; Hadjiargyrou, M. *Biomaterials* **2003,** *24*, 4977.
33. Li, D.; Fery, M. W.; Baeumner, A. J. *J. Membr. Sci.* **2006,** *279*, 354.
34. Agarwal, S.; Wendorff, J. H.; Greiner, A. *Polymer* **2008,** *49*, 5603.
35. Wen, Y. H.; Lin, H. C.; Li, C. H.; Hua, C. C. *Polymer* **2004,** *45*, 8551.
36. Wang, C.; Cheng, Y. W.; Hsu, C. H.; Chien, H. S.; Tsou, S. Y. *J. Polym. Res.* **2011,** *18*, 111.
37. Pötschke, P.; Abdel-Goad, M., Alig, I.; Dudkin, S.; Lellinger, D. *Polymer* **2004,** *45*, 8863.
38. Anderson, K. S.; Hillmyer, M. A. *Macromoleculers* **2004,** *37*, 1857.
39. Rayment, P.; Ross-Murphy, S. B.; Ellis, P. R. *Carbohydr. Polym.* **2000,** *43*, 1.
40. Sung, J. H.; Kim, H. S.; Jin, H. J.; Choi, H. J.; Chin, I. J. *Macromolecules* **2004,** *37*, 9899.
41. Seoul, C.; Kim, Y. T.; Baek, C. K. *J. Polym. Sci. Part B* **2003,** *41*, 1572.
42. Huang, C. L.; Wang, C. *Euro. Polym. J.* **2011,** *47*, 2087.
43. Pan, P.; Kai, W.; Zhu, B.; Dong, T.; Inoue, Y. *Macromolecules* **2007,** *40*, 6898.
44. Zhang, J.; Duan, Y.; Sato, H.; Tsuji, H.; Noda, I.; Yan, S.; Ozaki, Y. *Macromolecules* **2005,** *38*, 8012.
45. Yu, Z.; Chen, D.; Tøtdal, B.; Zhao, T.; Dai, Y.; Yuan, W.; Holmen, A. *Appl. Cata. A* **2005,** *279*, 223.
46. Inai, R.; Kotaki, M.; Ramakrishna, S. *Nanotechnology* **2005,** *16*, 208.
47. Hu, X.; An, H.; Li, Z. M.; Geng, Y.; Li, L.; Yang, C. *Macromolecules* **2009,** *42*, 3215.
48. Norris, I. D.; Shaker, M. M.; Ko, F. K.; MacDiarmid, A. G. *Synth. Met.* **2000,** *114*, 109.
49. Laforgue, A.; Robitaille, L. *Synth. Met.* **2008,** *158*, 577.
50. Laforgue, A.; Robitaille, L. *Macromolecules* **2010,** *43*, 4194.
51. Ounaies, Z.; Park, C.; Wise, K. E.; Siochi, E. J.; Harrison, J. S. *Compos. Sci. Technol.* **2003,** *63*, 1637.
52. Kim, H. S.; Jin, H. J.; Myung, S. J.; Kang, M.; Chin, I. J. *Macromol. Rapid. Commun.* **2006,** *27*, 146.
53. Kirkpatrick, S. *Rev. Mod. Phys.* **1973,** *45*, 574.
54. Logakis, E.; Pandis, Ch.; Pissis, P.; Pionteck, J.; Pötschke, P. *Compos. Sci. Technol.* **2011,** *71*, 854.
55. Zong, X.; Ran, S.; Kim, K. S.; Fang, D.; Hsiao, B. S.; Chu, B. *Biomacromolecules* **2003,** *4*, 416.
56. Heaney, M. B. *Phys. Rev. B* **1995,** *52*, 12477.
57. Batrouni, G. G.; Hansen, A.; Larson, B. *Phys. Rev. E* **1996,** *53*, 2292.
58. Vionnet-Menot, S., Grimaldi, C.; Maeder, T.; Strässler, S.; Ryser, P. *Phys. Rev. B* **2005,** *71*, 064201, 1.
59. Rubin, Z.; Sunshine, S. A.; Heaney, M. B.; Bloom, I.; Balberg, I. *Phys. Rev. B* **1999,** *59*, 12196.
60. Dalmas, F.; Dendievel, R.; Chazeau, L.; Cavaillé, J. Y.; Gauthier, C. *Acta. Mater.* **2006,** *54*, 2923.
61. McLachlan, D. S.; Heiss, W. D.; Chiteme, C.; Wu, J. *Phys. Rev. B* **1998,** *58*, 13558.
62. Lu, W.; Lin, H.; Chen, G. *J. Polym. Sci. Part B* **2006,** *44*, 1846.
63. Huang, C. L.; Wang, C. *Carbon* **2011,** *49*, 2334.